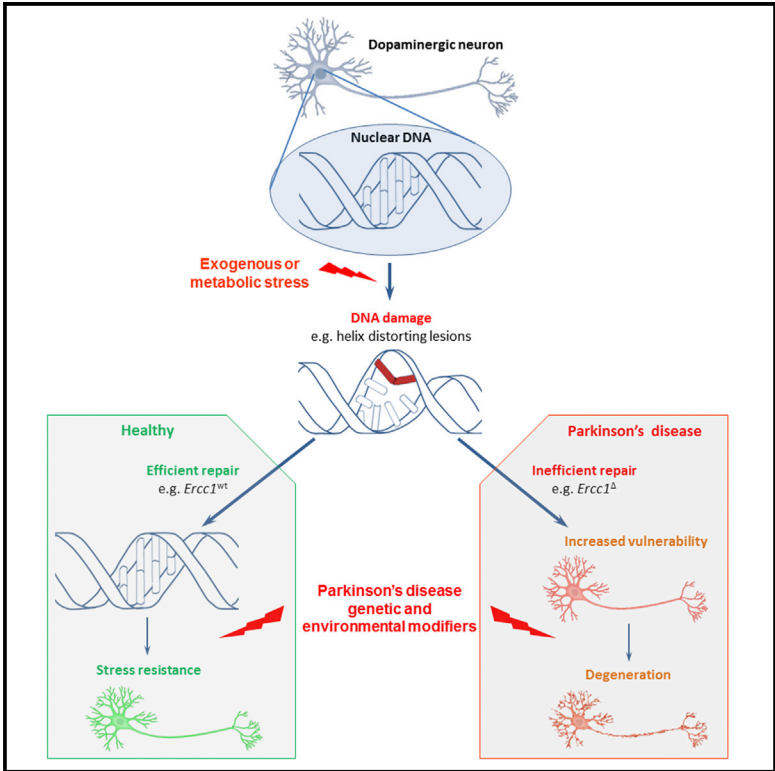


Inefficient DNA Repair Is an Aging-Related Modifier of Parkinson’s Disease

Graphical Abstract



Authors

Sara Sepe, Chiara Milanese, Sylvia Gabriels, ..., Fabio Blandini, Jan H.J. Hoeijmakers, Pier G. Mastroberardino

Correspondence

p.g.mastroberardino@erasmusmc.nl

In Brief

Sepe et al. demonstrate that the nucleotide excision repair (NER) gene *Ercc1* is essential for dopaminergic neuronal integrity. Mild *Ercc1* dysfunction is sufficient to elicit Parkinson’s disease (PD)-related dopaminergic pathology and to sensitize to PD-associated toxins. Furthermore, they show that PD patients’ peripheral cells are characterized by inefficient NER.

Highlights

- *Ercc1*-mediated DNA repair is necessary for preservation of dopaminergic neurons
- Mouse mutants with mild *Ercc1* defects display signs of dopaminergic pathology
- Mild *Ercc1* dysfunction is sensitized to the prototypical PD neurotoxin MPTP
- PD patients’ peripheral cells exhibit inefficient nucleotide excision repair

Accession Numbers

GSE75000



Inefficient DNA Repair Is an Aging-Related Modifier of Parkinson's Disease

Sara Sepe,¹ Chiara Milanese,^{1,2} Sylvia Gabriels,¹ Kasper W.J. Derks,¹ Cesar Payan-Gomez,^{1,3} Wilfred F.J. van IJcken,⁴ Yvonne M.A. Rijksen,¹ Alex L. Nigg,⁵ Sandra Moreno,⁶ Silvia Cerri,⁷ Fabio Blandini,⁷ Jan H.J. Hoeijmakers,¹ and Pier G. Mastroberardino^{1,*}

¹Department of Molecular Genetics, Erasmus Medical Center, 3015 Rotterdam, the Netherlands

²Ri.Med Foundation, 90133 Palermo, Italy

³Facultad de Ciencias Naturales y Matemáticas, Universidad del Rosario, 111711 Bogotá, Colombia

⁴Center for Biomics, Erasmus Medical Centre, 3015 Rotterdam, the Netherlands

⁵Optical Imaging Center, Erasmus Medical Centre, 3015 Rotterdam, the Netherlands

⁶University of "Roma Tre," 00146 Rome, Italy

⁷Laboratory of Functional Neurochemistry, Center for Research in Neurodegenerative Diseases, C. Mondino National Neurological Institute, 27100 Pavia, Italy

*Correspondence: p.g.mastroberardino@erasmusmc.nl
<http://dx.doi.org/10.1016/j.celrep.2016.04.071>

SUMMARY

The underlying relation between Parkinson's disease (PD) etiopathology and its major risk factor, aging, is largely unknown. In light of the causative link between genome stability and aging, we investigate a possible nexus between DNA damage accumulation, aging, and PD by assessing aging-related DNA repair pathways in laboratory animal models and humans. We demonstrate that dermal fibroblasts from PD patients display flawed nucleotide excision repair (NER) capacity and that *Ercc1* mutant mice with mildly compromised NER exhibit typical PD-like pathological alterations, including decreased striatal dopaminergic innervation, increased phospho-synuclein levels, and defects in mitochondrial respiration. *Ercc1* mouse mutants are also more sensitive to the prototypical PD toxin MPTP, and their transcriptomic landscape shares important similarities with that of PD patients. Our results demonstrate that specific defects in DNA repair impact the dopaminergic system and are associated with human PD pathology and might therefore constitute an age-related risk factor for PD.

INTRODUCTION

Parkinson's disease (PD) is a common neurodegenerative disorder deranging the nigro-striatal circuits of the brain and particularly dopaminergic (DA) neurons in the substantia nigra pars compacta (SNpc). PD pathogenesis is complex and includes alterations in multiple biological pathways. Defects in protein quality and folding control, which culminate in the accumulation of insoluble proteinaceous aggregates principally composed of alpha-synuclein (α -syn), are critical in the disease progression.

Additional cardinal features of PD pathobiology are bioenergetic anomalies—and specifically defects in mitochondrial respiratory complex I (C-I)—and altered oxido-reductive (redox) state (Greenamyre and Hastings, 2004). Simultaneous perturbation of these pathways in specific functional domains of the brain (e.g., the nigro-striatal system) constitutes a functional signature of the disorder and a reference for modeling in laboratory animals.

The vast majority of PD cases are idiopathic (typical PD), and etiology is likely to be due to complex synergistic interactions between environmental factors—for instance, pesticide exposure (Kamel et al., 2007)—and predisposing genotypes (GxE interactions). The outcome of these interactions might be exacerbated by aging, the single most important risk factor for PD (Chinta et al., 2013; Collier et al., 2011). Studies on aging, however, are laborious and extremely time-consuming, and consequently, the specific molecular mechanisms underlying increased risk for PD later in life remain largely unknown.

Aging is intrinsically associated with time-dependent accumulation of macromolecular damage. Although the latter interests virtually all biomolecules, accumulation of lesions in DNA is particularly relevant. DNA is, in fact, at the apex of biological information hierarchy, and its modification can result in lasting, transmittable, adverse consequences. Accordingly, DNA is the sole biomolecule that can be repaired when damaged. Experimental evidence in mutant mouse models and humans demonstrated that derangement of specific DNA repair systems results in dramatically accelerated wide-spread aging phenotypes and progeroid syndromes that recapitulate essential features of natural aging, albeit with a faster progression rate (Hoeijmakers, 2009).

The nucleotide excision repair (NER) system corrects forms of DNA damage that cause severe structural deformations in the double-helix, which can be caused by a remarkably diverse range of lesions: UV-induced cyclobutane pyrimidine dimers and 6-4 photoproducts; numerous chemical adducts; DNA-protein cross-links; intra-strand cross-links; and some forms of

oxidative DNA damage (D'Errico et al., 2006; Nospikel, 2008). NER therefore constitutes the most-versatile repair mechanism, and it is not surprising that congenital NER defects result in harsh deterioration of cellular functions, leading to severe disorders. On a molecular level, NER is orchestrated as a multi-step mechanism, composed of two converging branches: global genome- and transcription coupled-NER (GG-NER and TC-NER, respectively). GG-NER repairs an ample spectrum of helix-distorting lesions genome-wide, whereas TC-NER repairs lesions that block RNA polymerase and prevent transcription elongation. Defects in GG-NER, which underlie xeroderma pigmentosum (XP), lead to broadly diffused accumulation of damage, enhanced insurgence of mutations predisposing to (skin) cancer, and neurological abnormalities in later life. Conversely, defects in TC-NER interfere with a highly active process, transcription, and elicit profound functional alterations favoring cell death over carcinogenesis. In this case, the clinical outcome is dramatic, as in Cockayne syndrome (CS), and includes drastic neurodevelopmental defects and accelerated aging (Hoeijmakers, 2009). Emerging evidence showing that NER also participates in the repair of oxidative DNA damage might be of particular relevance for DA neurons in view of their physiologically oxidized intracellular environment and of their pronounced vulnerability to pro-oxidant insults (Guzman et al., 2010; Horowitz et al., 2011).

Here, we investigated the nexus between aging and PD by evaluating the possibility that defective NER might participate to the etiopathology of this insidious disorder.

RESULTS

The collection of signs associated with NER defects includes neurological symptoms in both humans and laboratory models, and current experimental evidence supports the notion that imperfect NER might constitute a general mechanism of neurodegeneration (Niedernhofer, 2008; Sepe et al., 2013). It is unclear, however, whether NER derangement specifically contributes to chronic neurodegeneration disorders and particularly to PD. Moreover, NER relevance for the preservation of nigrostriatal DA circuits has never been interrogated.

In silico analysis of expression profile datasets from open repositories indicated that several NER genes are expressed in the human SNpc (Sepe et al., 2013), yet functional evidence determining NER importance for DA neurons was lacking. The latter was assessed in a conditional mouse model with targeted deletion of the key DNA repair gene *Ercc1* in DA neurons. *Ercc1* associates with its partner *XPF* to form an endonuclease central to NER, and its ablation completely inactivates the pathway (Weeda et al., 1997). Whereas *Ercc1* has accessory functions in other pathways than NER, the latter remains its main domain of action. Moreover, mutations in *Ercc1* cause a progeroid phenotype in also rodents, which does not manifest when pure NER genes (e.g., XPA) are deleted, and *Ercc1* mutants are therefore informative models to investigate age-related genomic instability to PD. Cre-recombinase:*loxP* (Cre-*loxP*) system was used to generate mutants with targeted deletion in dopamine transporter (DAT)-expressing neurons. Specificity of Cre recombinase activity was validated using a *lacZ* reporter

that confirmed expression in DA neurons of the SNpc and not in other cell types, such as serotonergic neurons of the Raphe nucleus (Figure S1).

Ercc1^{-/-}DAT-Cre⁺ mice are viable and normal at birth. At 26 weeks of age, specific deletion of *Ercc1* in DA neurons mice elicits reduction in tyrosine hydroxylase (TH) immunoreactivity in the SNpc and in the striatum (Figures 1A and 1B). Aging profoundly exacerbates SNpc DA neurons reduction, as evidenced in 52-week-old *Ercc1*^{-/-}DAT-Cre⁺ mice (Figure 1C). Damage is limited in DA neurons and other populations remain unaffected, as indicated by unchanged NeuN immunoreactivity (Figures 1A and 1B). Overall, these findings demonstrate that *Ercc1* function and NER are essential to preserve integrity of the DA circuits in time.

Ercc1^{-/-}DAT-Cre⁺ mice provided proof-of-concept evidence that *Ercc1* function and NER are indispensable for the DA system and might therefore be also relevant for PD. Data on patients' peripheral cells, however, indicate that, in human PD, biological anomalies are rather systemic (Schapira et al., 1989) and this feature is not recapitulated in the *Ercc1*^{-/-}DAT-Cre⁺ knockout model, where the defect is confined to DA neurons. Whole-body *Ercc1* mutants, instead, might provide better information on the human disorder. Complete ablation of *Ercc1*, however, results in an extremely aggressive phenotype modeling pathologies such as XP and CS (Hoeijmakers, 2009). These diseases manifest in childhood, proceed rapidly, and have a very different clinical presentation than that observed in late-onset, slow-progressing neurodegenerative disorders. We therefore focused on a strain expressing one mutated allele, which generates a severely, albeit not fully dysfunctional, truncated form of *Ercc1*, in combination with a wild-type allele (*Ercc1*^{Δ/+}). This particular strain lacks an overt phenotype, has normal lifespan, and thus constitutes a more-representative platform to investigate the chronic, slow-progressing pathology of PD. At an age in which wild-type animals do not present any DA alteration (20 weeks), *Ercc1*^{Δ/+} mice already display functional evidence of DA injury and decreased striatal DA innervation in particular (Figure 2A). The latter is not paralleled by decreased DA number in the SNpc (Figure 4B), and expression of the DA rate-limiting enzyme TH protein expression is increased in *Ercc1*^{Δ/+} DA cell bodies (Figure 2A). These observations suggest that this model features an early and pre-symptomatic derangement of the DA system in which only striatal terminals are affected and compensatory mechanisms are ongoing (Greenwood et al., 1991).

Analyses of additional molecular indicators of PD progression confirm ongoing DA dysfunction in *Ercc1*^{Δ/+}. Because PD is intrinsically associated with increased oxidation of the thiol/disulfide redox couple in DA neurons (Mastroberardino et al., 2008, 2009), these equilibria were studied in *Ercc1*^{Δ/+} at single-cell level, using imaging methods we previously developed (Horowitz et al., 2011). SNpc DA neurons are indeed more oxidized in *Ercc1*^{Δ/+} (Figure 2B) whereas no sign of increased oxidation was detected in hippocampal or Purkinje's neurons (Figure S2A). These perturbations are paralleled by increased γ H2AX foci, specifically in DA neurons, confirming both augmented DNA damage in *Ercc1*^{Δ/+} and the relevance of *Ercc1* in double-strand breaks (DSB) repair in vivo (Figure 2C). *Ercc1*^{Δ/+} mice also present increased ubiquitination levels and thus defects in protein homeostasis, albeit not

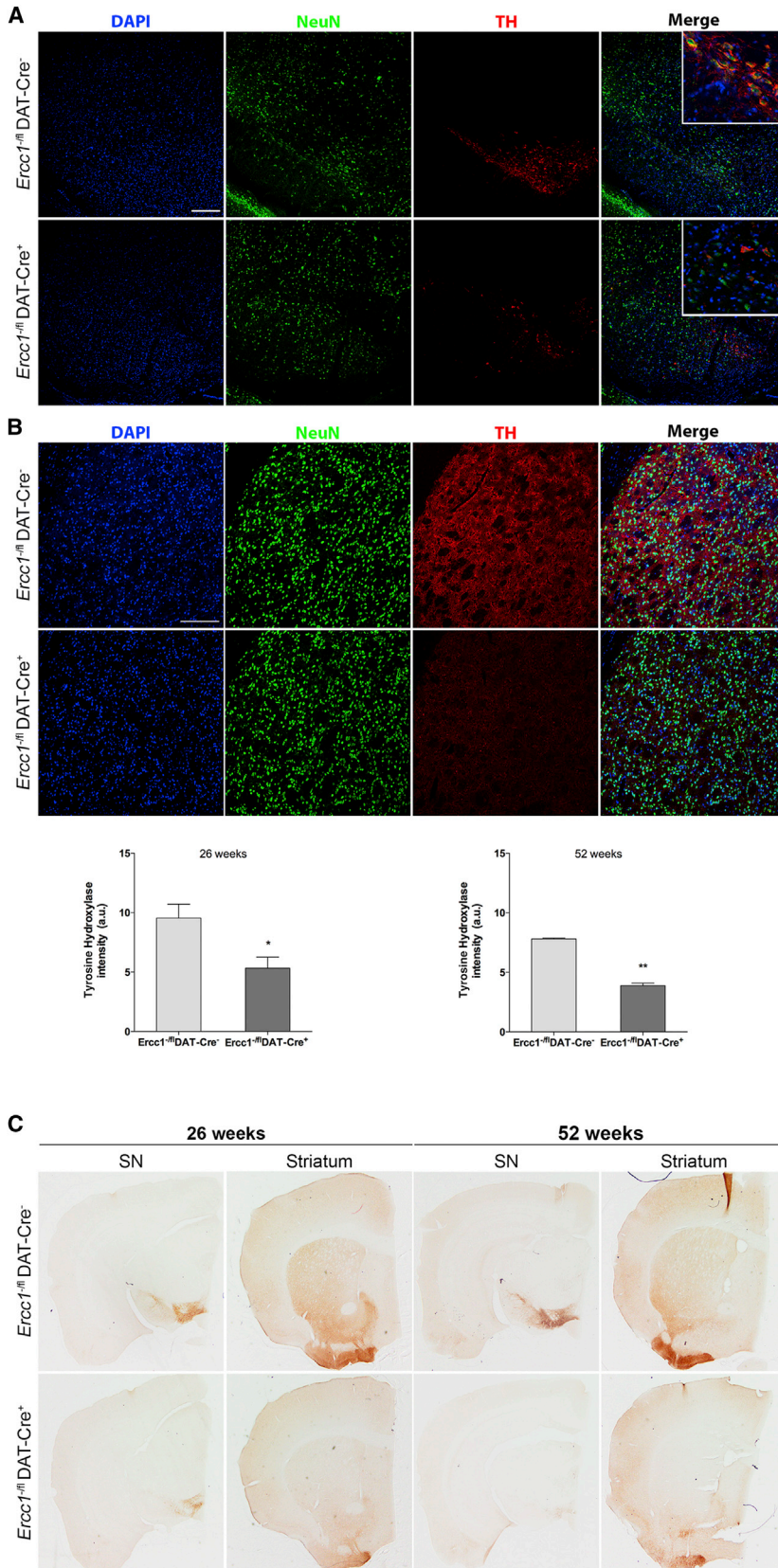


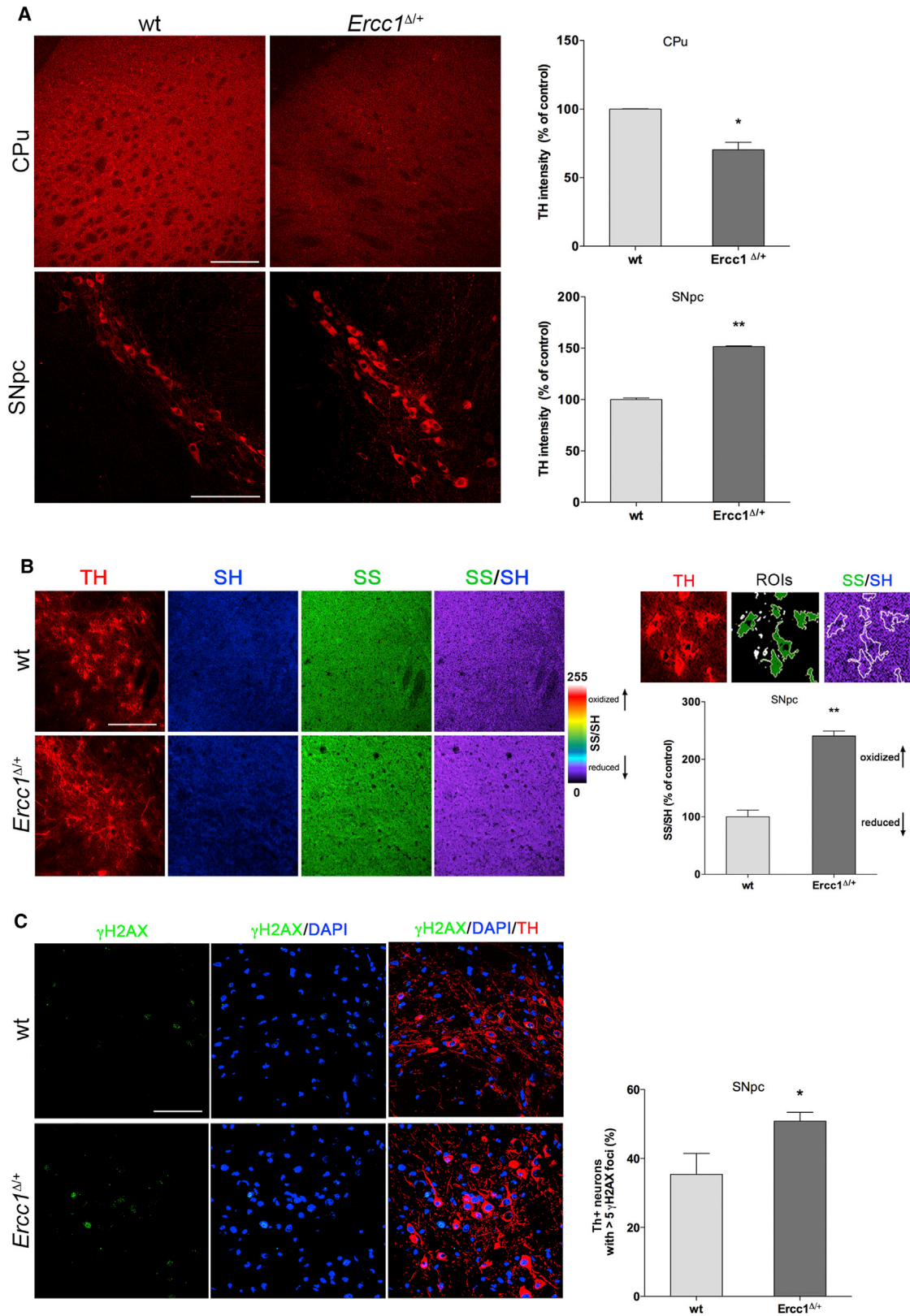
Figure 1. NER Is Essential for the Integrity of the DA System

(A) Targeted deletion of the key NER gene *Ercc1* in DA neurons results in degeneration of striatal DA processes already evident in 26-week-old mice; DA neurons (red) and the general neuronal population (green) were revealed with anti-TH and anti-NeuN antibodies, respectively. Inset shows clear reduction of TH⁺ neurons in mutants.

(B) Loss of nigral DA neurons is paralleled by reduced TH immunoreactivity in mutants' striatum. Bar graphs illustrate quantification of striatal TH immunoreactivity.

(C) Reduced TH⁺ neurons in SNpc and decreased striatal TH immunoreactivity is exacerbated at 52 weeks of age.

The scale bar represents 200 μm (A), 500 μm (B), and 1,000 μm (C). Error bars on the graph denote SEM. Six 26- and 52-week-old animals from each genotype were used for each experiment.



(legend on next page)

exclusively in DA neurons and without impairment of proteasomal activity (Figure 3A; see also Figure S2C). Conversely, total α -syn levels are unchanged (Figure S2B). However, levels of phosphorylated α -syn (p129S), which is the most-represented modified species of α -syn within PD pathological inclusions (Anderson et al., 2006), are higher in *Ercc1*^{Δ/+} SNpc (Figure 3B). These alterations are paralleled by more-general signs of pathology such as increased astrocyte activation in the SNpc and in the striatum of mutant animals (Figures S3A and S3B).

Given the relevance of mitochondrial C-I defects in the etiology of PD, its activity was evaluated in *Ercc1*^{Δ/+} mice by measuring glutamate-malate-supported respiration in organelles extracted from the ventral mesencephalon (VM). Both basal (i.e., state 2 = state 4) and ADP-stimulated (i.e., state 3) respiration is decreased in mutants (Figure 3C). Defects concern specifically C-I because complex-II-driven respiration (i.e., supported by succinate) is higher in *Ercc1*^{Δ/+} (Figure 3D), suggesting ongoing compensatory mechanisms. Electron micrographs revealed that functional defects are paralleled by morphological abnormalities in *Ercc1*^{Δ/+} DA neurons' mitochondria (Figure 3E).

Next-generation RNA sequencing (RNA-seq) and canonical pathway analysis provided further mechanistic insights on the consequences of NER inefficiency in the VM. RNA-seq revealed 460 differentially expressed genes (DEGs), 187 of which were up- and 273 downregulated in *Ercc1*^{Δ/+} when compared to matched wild-type controls. RNA-seq data were validated with qPCR on 12 significantly up- or downregulated genes randomly chosen among the most-significantly altered pathways (Figure S4; see also Table S3).

Differences between expression profiles of *Ercc1*^{Δ/+} and wild-type matched controls were determined using overrepresentation analysis (ORA) to highlight the significantly altered specific functional categories (Figure 3F). As expected, the NER pathway is downregulated in *Ercc1*^{Δ/+} (Figure 3G). Other modified pathways included highly relevant processes for PD, including oxidative phosphorylation, mitochondrial dysfunction, and proteasome. Transcriptomic analysis therefore provided a strong unbiased confirmation of the functional results obtained in our experiments, showing altered intracellular redox state, bioenergetics defects, (Figures 2B and 3C, respectively), and increased ubiquitination levels (Figure 3A). Interestingly, a recent report has demonstrated the involvement of EIF2-signaling pathway, which constitutes the hit with highest significance in our analysis (Table S1), in both genetic and sporadic forms of the disease (Mutez et al., 2014). Overall, these results further strengthen the concept that inefficient NER affects biological processes relevant for the DA system integrity.

The fundamental issue as to whether this specific combination of pathways' alterations reverberates human pathology, however, remained to be addressed. We therefore performed gene

set enrichment analysis (GSEA) using gene collections as defined by the Kyoto Encyclopedia of Genes and Genomes (KEGG) and reducing intrinsic redundancy in pathways databases. We compared *Ercc1*^{Δ/+} RNA-seq dataset with publicly available datasets from human PD and incidental Lewy body disease (ILBD) SNpc, which is regarded as a pre-symptomatic form of PD (DelleDonne et al., 2008). Of the 12 pathways downregulated in *Ercc1*^{Δ/+}, five are shared with ILBD and/or PD and include very relevant processes for PD, such as oxidative phosphorylation, glutathione metabolism, and proteasome (Figure 3G). As expected, the gene set KEGG_PARKINSONS_DISEASE (<http://www.broadinstitute.org>), which was consolidated with the KEGG_HUNTINGTONS_DISEASE pathway after redundancy reduction, is downregulated in all datasets, further emphasizing objective affinities between our mouse model and the human disease. Of the 17 upregulated pathways in *Ercc1*^{Δ/+}, seven are shared with PD and none with ILBD. Of note, only one pathway is shared between ILBD and PD (Figure 3H). Common upregulated pathways include inflammation and mitogen-activated protein kinase (MAPK) signaling, which are both very relevant for human PD (Deleidi and Gasser, 2013; Horowitz et al., 2011; Lin et al., 2008). In summary, transcriptomics analyses highlight important molecular similarities between *Ercc1*^{Δ/+} mice and the human disease and substantiate our findings showing functional alterations in mitochondrial function, intracellular redox state, and increased ubiquitination in the VM.

Enrichment factors calculation (EF) was used to explore further affinities between *Ercc1*^{Δ/+} and human PD. EF estimates similarity between datasets by comparing the extent of abundance of common elements in the groups under consideration (e.g., *Ercc1*^{Δ/+} and PD) with the extent of abundance that would be expected in random groups. The number of common downregulated pathways in related pathologies such as PD and ILBD is 4.2 times more abundant than what expected by chance ($p < 10^{-7}$; Table S2). Downregulated pathways common to *Ercc1*^{Δ/+} and PD and to *Ercc1*^{Δ/+} and ILBD are, respectively, 6.7 and 5.6 more abundant than what would be expected by chance ($p < 10^{-4}$). We did not observe a significant enrichment in upregulated processes shared between *Ercc1*^{Δ/+} and ILBD, whereas we did observe a 2-fold enrichment ($p < 0.0005$) when comparing *Ercc1*^{Δ/+} and PD. As expected, the number of common upregulated pathways between both PD and ILBD human datasets was 9.2 times more abundant than what would be expected by chance ($p < 10^{-4}$). These additional analyses further confirm affinities between the transcriptional landscape of *Ercc1*^{Δ/+} and human PD.

Elements such as (1) decreased striatal TH innervation without significant differences in DA nigral cell bodies, (2) increased phospho-synuclein levels without detectable aggregates, and

Figure 2. Alterations in the Nigro-striatal DA System in *Ercc1*^{Δ/+} Mice

(A) Decreased striatal DA innervation in the *caudate putamen* (CPU) of *Ercc1*^{Δ/+} mice is paralleled by increased TH expression in SNpc neuronal bodies. Graphs on the right side represent the quantification of the fluorescent signal.

(B) Increased oxidation in the SS/SH redox couple in SNpc DA neurons. The montage on the right side represents a zoom showing how the Metamorph software automatically defines regions of interest (ROIs) by using the TH signal as a mask. ROIs are then transferred to the image expressing the SS/SH ratio.

(C) *Ercc1*^{Δ/+} mutants feature increased DNA damage as indicated by the higher proportion of DA neurons containing more than five γ H2AX foci per nucleus. The scale bar represents 500 μ m (A) and 150 μ m (B). * $p < 0.05$; ** $p < 0.01$; unpaired t test. Error bars on the graph denote SEM. Six 20-week-old animals from each genotype were used in each experiment.

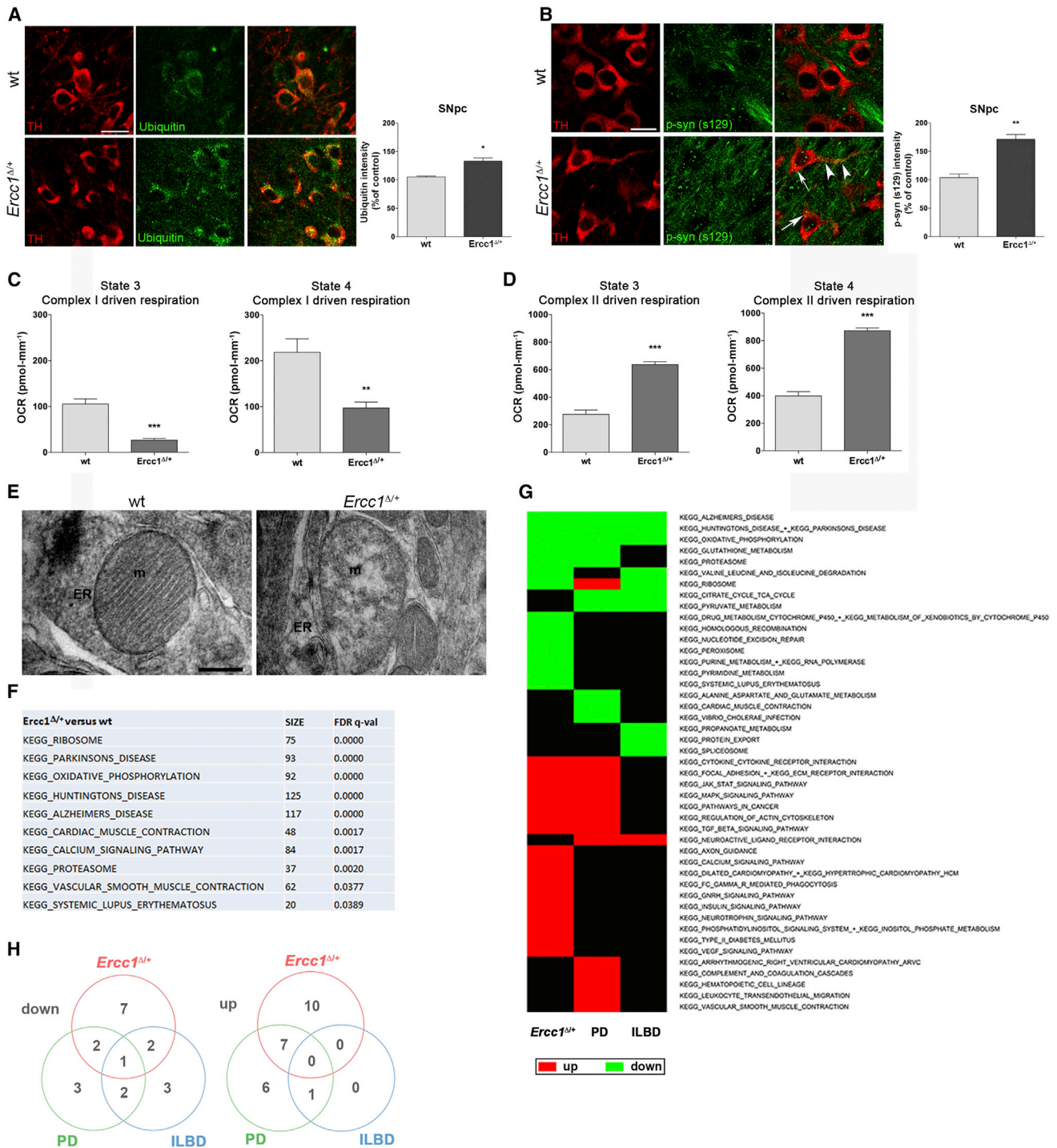


Figure 3. *Ercc1*^{Δ/+} Mice Display Hallmarks of PD Pathology and Share Similarities with PD Patients

(A) Increased ubiquitination in the SNpc and in its DA neurons. The corresponding graph expresses intensity of the ubiquitin signal in TH⁺ regions of the image. (B) Increased phosphorylation of α -syn at ser129 (p-syn) in both cell bodies (arrows) and processes (arrowheads) of SNpc DA neurons. Graph expresses intensity of the p-syn signal in TH⁺ regions.

(C) Impaired C-I-driven mitochondrial respiration in *Ercc1*^{Δ/+} mice. When energized with glutamate/malate, mitochondria extracted from the VM region of *Ercc1*^{Δ/+} mice exhibit decreased respiration in both state 4 and state 3.

(D) Conversely, succinate-stimulated respiration is increased in both state 4 and state 3 in mitochondria extracted from the VM region of *Ercc1*^{Δ/+} animals.

(E) Ultrastructural electron microscopy reveals abnormal mitochondria with disorganized cristae in *Ercc1*^{Δ/+} SNpc DA neurons. DA neurons are unambiguously identified by precipitated electron-dense DAB resulting from pre-embedding TH immunostaining. ER, endoplasmic reticulum; M, mitochondria.

(legend continued on next page)

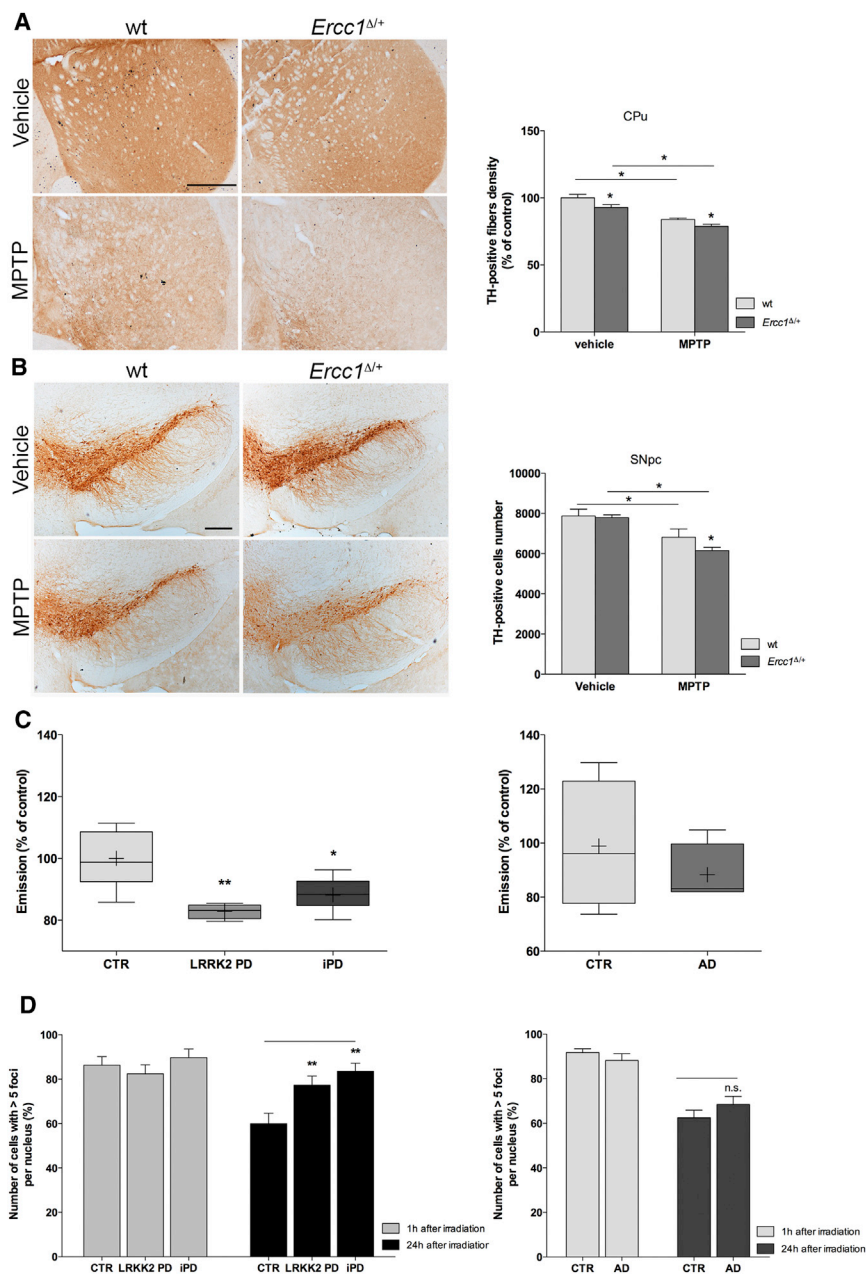


Figure 4. Increased Sensitivity of *Ercc1*^{Δ/+} Mice to MPTP and Inefficient NER in PD Patients' Fibroblasts

(A) Decrease in striatal DA innervation induced by MPTP treatment is more pronounced in *Ercc1*^{Δ/+} mice.

(B) Unbiased stereological counts indicating more severe MPTP-induced DA loss in *Ercc1*^{Δ/+} mice. The scale bar represents 500 μ m (A) and 200 μ m (B). **p* < 0.05; two-way ANOVA. Error bars on the graph denote SEM. For the experiment, five 20-week-old animals for each group were used.

(C) Mild NER defects in fibroblasts derived from idiopathic (iPD; *n* = 11) and genetic (LRRK2-PD; *n* = 4) PD patients, but not from AD cases, as measured by UDS assay. Genetic PD cells harbor either the G2019S (*n* = 2) or the R1441G (*n* = 2) mutation. **p* < 0.05; ***p* < 0.01; one way ANOVA. No significant differences were detected in cells derived from AD patients (*n* = 4). Box and whiskers representation also shows the mean of the values (+).

(D) DSB repair efficiency was evaluated in PD and AD fibroblasts. PD cases did not differ from control cases 1 hr after exposure to gamma irradiation (2 Gy), whereas they exhibited a significant increase in the number γ H2AX foci still present 24 hr after irradiation (left graph), which suggests impaired DSB repair capacity. AD cases did not present significant differences from respective, matched controls **p* < 0.05; two-way ANOVA. Error bars on graph represent SEM.

pyridine (MPTP). As expected, 3 days MPTP treatment induced a significant decrease in striatal TH immunoreactivity as well as in DA neuronal bodies in the SNpc (Figures 4A and 4B). Neurodegeneration, however, was more pronounced in *Ercc1*^{Δ/+}, which suffered a 12% loss in nigral DA cell number when compared to vehicle-treated littermates, against the 7.5% loss observed in wild-type animals. Of note, the extent of degeneration in these experiments, which are performed in a genetically uniform C57BL/6:FVB F1 hybrid background, is in agreement with previous reports indicating

(3) absence of overt symptoms suggest that *Ercc1*^{Δ/+} mice might represent a pre-symptomatic model predisposed to DA degeneration upon detrimental GxE interactions. To explore possible synergies between ineffective DNA repair and environmental chemicals associated with PD, we exposed *Ercc1*^{Δ/+} mice to the prototypical PD toxin 1-methyl-4-phenyl-1,2,3,6-tetrahydro-

MPTP resistance in the FVB background (Liu et al., 2003). DA innervation in the striatum after MPTP was also lower in *Ercc1*^{Δ/+}.

The possibility that NER may be functionally deranged in human PD was finally evaluated by assaying unscheduled DNA synthesis (UDS) in patients. UDS quantifies NER by monitoring

(F) RNA-seq and subsequent canonical pathway analysis reveals that pathways highly relevant for PD pathogenesis are altered in *Ercc1*^{Δ/+} VM.

(G) Heatmap comparing downregulated (green) and upregulated (red) pathways in *Ercc1*^{Δ/+} mice, in PD, and in ILBD.

(H) Venn diagrams showing the number of common downregulated and upregulated pathways in *Ercc1*^{Δ/+}, PD, and human ILBD.

The scale bar represents 15 μ m (A and B) and 0.6 μ m (C). **p* < 0.05; ****p* < 0.001; ***p* < 0.01; unpaired *t* test. Error bars on the graph denote SEM. Six (A, B, and E) to eight (C and D) 20-week-old animals for each genotype were used in each experiment.

DNA synthesis after damage in cells outside S phase, therefore in stages in which DNA synthesis is unambiguously associated with repair. DNA damage is generated by UV-C exposure (16 J/m^2), which creates lesions specifically amended by NER: 6-4 photoproducts and pyrimidine dimers. DNA synthesis is measured by incorporation of labeled precursors that can be subsequently detected using copper(I)-catalyzed azide-alkyne cycloaddition (or “click chemistry”) of fluorescent molecules (Salic and Mitchison, 2008). UDS revealed reduced NER capacity in both idiopathic and genetic (LRRK2 G2019S or R1441G) patients, particularly in those carrying the LRRK2 mutation (Figure 4C; see also Table S4). Of note, this magnitude of UDS decrease is comparable to that previously reported in *Ercc1*^{Δ/+} fibroblasts (Weeda et al., 1997) and further substantiates the affinities between this mouse strain and PD. Conversely, fibroblasts from AD patients do not exhibit any significant difference in NER capacity, at least under these conditions (Figure 4D).

DNA repair pathways functionally interact and, for instance, the critical NER gene *Ercc1* also facilitates DNA DSB and inter-strand cross-link repair (Ahmad et al., 2008). We therefore analyzed how these specific lesions are repaired in PD and Alzheimer’s disease (AD) fibroblasts by evaluating the number of γH2AX foci after gamma irradiation. Whereas we did not observe differences in the formation of foci between the different groups, PD fibroblasts exhibited decreased DSB repair capacity, evidenced by the persistence of foci 24 hr after irradiation (Figure 4D). Overall, these results demonstrate a systemic defect in DNA repair in PD patients.

DISCUSSION

Traditionally, investigations on DNA damage and PD have been circumscribed to mtDNA, whereas nuclear DNA (nuDNA) only received modest attention. Impact of nuDNA lesions’ on cell function, however, may largely exceed that of mtDNA damage. nuDNA is in fact present in a single copy, whereas cells contain hundreds of mtDNA copies, and in post-mitotic neurons, nuDNA integrity must be preserved lifelong. Here, we demonstrate that the presence of a truncated *Ercc1* allele is sufficient to cause mild derangement of the nuDNA repair machinery in rodents, which in turn elicits anomalies typical of PD. Although *Ercc1* is involved in other DNA repair processes than NER, the latter remains its principal domain of action and it is therefore appropriate to infer that deranged NER is responsible, at least in part, for the observed PD-related anomalies in the DA system. Consistently, peripheral cells of genetic and idiopathic human PD cases display defective NER. It is, however, likely that other nuDNA repair pathways might participate to PD etiopathogenesis, and further studies will be necessary to achieve a full characterization. Nonetheless, our work addresses a gap concerning the relevance of nuDNA stability in PD and lays foundation for further investigations. Because deranged NER recapitulates essential aspects of natural aging in laboratory models and humans, our study also establishes a mechanistic nexus between PD and its principal risk factor.

Increased vulnerability of PD peripheral cells to DNA damage has been already described a long time ago in a study monitoring cell viability after X-rays exposure (Robbins et al., 1985). X-rays,

however, induce a broad spectrum of DNA lesions, including double- and single-strand breaks, and therefore do not allow identification of the specific defective repair pathway. UV-C, in contrast, circumscribes lesion type to bulky distortions, which are specifically amended by NER; on these premises, our experiments demonstrate unambiguously functional NER defects in PD. This evidence is of profound relevance given the causative association between NER and aging (Hoeijmakers, 2009), and it also implies that reduced NER efficiency could potentiate other detrimental GxE interactions to initiate pathogenesis. UDS experiments demonstrate that NER defects tend to be more pronounced in LRRK2 fibroblasts, which also display smaller variability when compared to cells from idiopathic cases. The reasons underlying these subtle differences are obscure and should be investigated in future studies. It is tempting to speculate, however, that mutations in LRRK2 might directly compromise the process of DNA repair. A recent report focused on mtDNA indeed established a link between LRRK2 mutations and DNA damage (Sanders et al., 2014a).

Further relevance of NER for the DA system integrity stems from its ability to amend also oxidative modifications in the double helix. Bulky structural distortions in DNA, which constitute the essential prerequisite for NER, can in fact also be caused by oxidative damage (D’Errico et al., 2006). In addition, recent reports demonstrate a cross-talk between NER and other repair pathways, including base excision repair, which is the preferred mechanism to correct oxidative lesions (Pascucci et al., 2011). Because of their distinctive physiology, DA neurons feature a relatively oxidized intracellular redox state, even in unstressed physiological conditions (Guzman et al., 2010; Horowitz et al., 2011), and PD pathogenesis is characterized by progressive oxidation of these cells (Mastroberardino et al., 2008). It is therefore conceivable that adequate repair systems to amend oxidative modifications are of particular importance to preserve genomic integrity in this specific neuronal population. Efficient repair of oxidative lesions has even greater significance in consideration of PD environmental risk factors, which principally include pro-oxidant pesticides (Kamel et al., 2007). Here, defective repair and consequent loss of fidelity in the genetic information could constitute modifiers sensitizing the DA system to environmental hazards and therefore predisposing to PD. Indeed, a very recent report demonstrates that oxidative mtDNA damage induced by the C-I inhibitor rotenone is detectable prior to any sign of degeneration (Sanders et al., 2014b). Our data demonstrate higher sensitivity of NER-deficient mice to the prototypical PD toxin MPTP and indicate that inefficient DNA repair may be a risk factor for PD. This is also supported by preliminary epidemiological investigations in small cohorts of idiopathic PD patients, demonstrating association with SNPs in some DNA repair genes (Cornetta et al., 2013; Gencer et al., 2012). At present, none of these variants interests genes in NER; the found variants, however, might certainly influence proper NER in consideration of complex cross-talk between the high number of proteins involved in DNA repair—some of which may have additional and often poorly characterized functions. Additional investigations focused on specific NER genes, and eventually analyzing cohorts with ascertained exposure to pro-oxidant pesticides, will unravel possible genetic associations with PD. Finally,

additional studies to determine synergism between mutations in genes associated with monogenic forms of PD (e.g., α -syn) and deranged NER are warranted.

In conclusion, our study demonstrated the relevance of nuDNA repair, and of NER in particular, for PD and suggests that aging-related genomic instability may constitute a genetic modifier predisposing to PD.

EXPERIMENTAL PROCEDURES

Human Dermal Fibroblasts

Primary human dermal fibroblasts from healthy and idiopathic PD patients were obtained as previously described (Ambrosi et al., 2014); clinical data are summarized in Table S4. Genetic PD (catalog ID ND32975, ND32976, ND32970, and ND33879) and AD fibroblasts and matched controls (catalog ID AG05810, AG07872, AG07936, AG08125, AG08269, AG08527, AG08543, and AG21158) were obtained from the Cell Repositories of the Coriell Institute for Medical Sciences (<http://ccr.coriell.org/sections/search/>).

UDS Assay

Cells were irradiated with UV-C 16 J/m² and then incubated with F10 medium supplemented with 10% dialyzed serum, 20 μ M 5-ethynyl-2'-deoxyuridine (EdU), and 1 μ M 5-fluoro-2'-deoxyuridine (FUrd) for 3 hr. Cells were then fixed and processed using the Click-iT EdU Alexa Fluor 594 Imaging Kit (Invitrogen).

DSB Analysis

Primary fibroblasts were seeded on glass coverslips at a concentration of 10⁵ cells/well and exposed to a 2 Gy γ -irradiation dose (Cesium-137 source; Gammacell 40 low-dose rate laboratory irradiator; Nordion). DSBs were detected using a mouse monoclonal anti-phospho-histone H2AX antibody (anti- γ H2AX - s139; 1:1,000; 05336; Millipore).

Animals

NER *Ercc1*^{Δ/+} mouse mutants generation and characterization has been previously described (Weeda et al., 1997). *Ercc1*^{Δ/+} mice are in a FVB:C57BL/6J (50:50) background. Animals were kept on a regular diet and housed at the Animal Resource Center (Erasmus University Medical Center), which operates in compliance with the "Animal Welfare Act" of the Dutch government, following the "Guide for the Care and Use of Laboratory Animals" as its standard.

MPTP Treatment

Mice were injected with 20 mg/kg of MPTP (M0986; Sigma-Aldrich) or saline (vehicle) intraperitoneally (i.p.) every 2 hr for a total of four injections, resulting in a cumulative dose of 80 mg/kg. Animals were sacrificed 3 days after treatment.

Immunofluorescence

Immunofluorescence (IF) was carried out according to standard procedures. Details and antibodies are described in Supplemental Experimental Procedures.

Electron Microscopy

Vibratome cut 100- μ m-thick sections were processed for immunocytochemistry with a mouse monoclonal anti-TH (1:4,000; Millipore; MAB318). Signal was revealed with 3,3'-diaminobenzidine (DAB). Slices were post-fixed in 1% OsO₄ and flat embedded in Epon 812 (TAAB). Ultrathin sections were obtained with a Reichert Ultracut S ultramicrotome, contrasted with uranyl acetate and lead citrate, and observed in a Philips CM120 electron microscope.

Thiol/Disulfide Histochemistry

Histological labeling of thiol/disulfides was performed as previously described (Horowitz et al., 2011).

Bioenergetics Assays

Bioenergetics assays were performed in an XF-24 Extracellular Flux Analyzer (Seahorse Bioscience), using 10 μ g of mitochondrial protein. C-I-driven respi-

ration was sustained by glutamate (2 mM) and malate (2 mM); complex-II-driven respiration was sustained by succinate (10 mM); in the latter case, rotenone (4 μ M) was added to inhibit C-I and prevent reversed electron transfer from succinate to nicotinamide adenine dinucleotide (NAD⁺).

mRNA Sequencing

Sample preparation from total RNA was performed using the TruSeq mRNA sample preparation kit (Illumina) according to the manufacturer's protocols and sequenced in one lane each of a HiSeq2500 (Illumina).

mRNA-Seq Analysis

Reads were aligned to the mouse reference genome (mm9) using Tophat (version 1.3.1.Linux_x86_64,-coverage-search, -butterfly-search,-segment-mismatches 1,-segment-length 18) via the NARWHAL (Brouwer et al., 2012) automation software. SAMMATE (<http://sammate.sourceforge.net/>; Xu et al., 2011) was used to detect and quantify transcripts. Gene counts were calculated taking into account the reads mapped on exons or on exon-exon junctions. DEGs were detected using the R package EdgeR (Robinson et al., 2010). An over-dispersed Poisson model was used to account for biological and technical variability. Genes with a false discovery rate (FDR) of <0.05 and fold change \pm 1.5 were considered to be differentially expressed.

Statistical Analysis

Experiments were performed in four to six independent biological replicates. Comparison of multiple groups was performed by ANOVA or Kruskal-Wallis test; comparisons between two groups were performed by t test.

ACCESSION NUMBERS

The accession number for the datasets reported in this paper is GEO: GSE75000.

SUPPLEMENTAL INFORMATION

Supplemental Information includes Supplemental Experimental Procedures, four figures, and four tables and can be found with this article online at <http://dx.doi.org/10.1016/j.celrep.2016.04.071>.

AUTHOR CONTRIBUTIONS

S.S. performed research with the help of C.M. and S.G. W.F.J.v.I. performed next-generation RNA-seq. K.W.J.D. assembled the NGS data, and C.P.-G. performed bioinformatics analyses. Y.M.A.R. generated the conditional mutants. A.L.N. assisted with 4Pi microscopy. S.C. and F.B. performed unbiased stereological counts. J.H.J.H. contributed to study design. P.G.M., S.S., and C.M. wrote the manuscript. All the authors provided intellectual input and overall assistance in designing and executing the study and in compiling the manuscript. P.G.M. conceived, designed, and directed the study.

ACKNOWLEDGMENTS

P.G.M. was supported by a grant from the Netherlands Genomics Initiative (NGI/NWO 05040202), a Marie Curie grant (IRG 247918), and the CEREBRAD grant under the EU-FP7 framework (project number 295552). The Extracellular Flux Analyzer by Seahorse Bioscience was purchased thanks to a generous donation from Dorpmans-Wigmans Stichting (to P.G.M.). J.H.J.H. acknowledges financial support from the NIH/National Institute of Aging (1P01 AG-17242-02), the National Institute of Environmental Health Sciences (1U01 ES011044), the Royal Academy of Arts and Sciences of the Netherlands (academia professorship), and a European Research Council Advanced Grant. C.M. was supported by the Ri.MED Foundation. The research leading to these results has received funding from the European Community's Seventh Framework Programme (FP7/2007-2013) under grant agreement no. HEALTH-F2-2010-259893. C.P.G. is supported by ERACOL.

Received: August 20, 2015

Revised: February 1, 2016

Accepted: April 19, 2016

Published: May 19, 2016

REFERENCES

- Ahmad, A., Robinson, A.R., Duensing, A., van Drunen, E., Beverloo, H.B., Weisberg, D.B., Hasty, P., Hoeijmakers, J.H., and Niedernhofer, L.J. (2008). ERCC1-XPF endonuclease facilitates DNA double-strand break repair. *Mol. Cell. Biol.* **28**, 5082–5092.
- Ambrosi, G., Ghezzi, C., Sepe, S., Milanese, C., Payan-Gomez, C., Bombardieri, C.R., Armentero, M.T., Zangaglia, R., Pacchetti, C., Mastroberardino, P.G., and Blandini, F. (2014). Bioenergetic and proteolytic defects in fibroblasts from patients with sporadic Parkinson's disease. *Biochim. Biophys. Acta* **1842**, 1385–1394.
- Anderson, J.P., Walker, D.E., Goldstein, J.M., de Laat, R., Banducci, K., Cacavello, R.J., Barbour, R., Huang, J., Kling, K., Lee, M., et al. (2006). Phosphorylation of Ser-129 is the dominant pathological modification of alpha-synuclein in familial and sporadic Lewy body disease. *J. Biol. Chem.* **281**, 29739–29752.
- Brouwer, R.W., van den Hout, M.C., Grosveld, F.G., and van Ijcken, W.F. (2012). NARWHAL, a primary analysis pipeline for NGS data. *Bioinformatics* **28**, 284–285.
- Chinta, S.J., Lieu, C.A., Demaria, M., Laberge, R.M., Campisi, J., and Andersen, J.K. (2013). Environmental stress, ageing and glial cell senescence: a novel mechanistic link to Parkinson's disease? *J. Intern. Med.* **273**, 429–436.
- Collier, T.J., Kanaan, N.M., and Kordower, J.H. (2011). Ageing as a primary risk factor for Parkinson's disease: evidence from studies of non-human primates. *Nat. Rev. Neurosci.* **12**, 359–366.
- Cornetta, T., Patrono, C., Terrenato, I., De Nigris, F., Bentivoglio, A.R., Testa, A., Palma, V., Poggioli, T., Padua, L., and Cozzi, R. (2013). Epidemiological, clinical, and molecular study of a cohort of Italian Parkinson disease patients: association with glutathione-S-transferase and DNA repair gene polymorphisms. *Cell. Mol. Neurobiol.* **33**, 673–680.
- D'Errico, M., Parlanti, E., Teson, M., de Jesus, B.M., Degan, P., Calcagnile, A., Jaruga, P., Bjorås, M., Crescenzi, M., Pedrini, A.M., et al. (2006). New functions of XPC in the protection of human skin cells from oxidative damage. *EMBO J.* **25**, 4305–4315.
- Deleidi, M., and Gasser, T. (2013). The role of inflammation in sporadic and familial Parkinson's disease. *Cell. Mol. Life Sci.* **70**, 4259–4273.
- DelleDonne, A., Klos, K.J., Fujishiro, H., Ahmed, Z., Parisi, J.E., Josephs, K.A., Frigerio, R., Burnett, M., Wszolek, Z.K., Uitti, R.J., et al. (2008). Incidental Lewy body disease and preclinical Parkinson disease. *Arch. Neurol.* **65**, 1074–1080.
- Gencer, M., Dasedemir, S., Cakmakoglu, B., Cetinkaya, Y., Varlibas, F., Tireli, H., Kucukali, C.I., Ozkok, E., and Aydin, M. (2012). DNA repair genes in Parkinson's disease. *Genet. Test. Mol. Biomarkers* **16**, 504–507.
- Greenamyre, J.T., and Hastings, T.G. (2004). Biomedicine. Parkinson's—divergent causes, convergent mechanisms. *Science* **304**, 1120–1122.
- Greenwood, C.E., Tatton, W.G., Seniuk, N.A., and Biddle, F.G. (1991). Increased dopamine synthesis in aging substantia nigra neurons. *Neurobiol. Aging* **12**, 557–565.
- Guzman, J.N., Sanchez-Padilla, J., Wokosin, D., Kondapalli, J., Ilijic, E., Schumacker, P.T., and Surmeier, D.J. (2010). Oxidant stress evoked by pacemaker in dopaminergic neurons is attenuated by DJ-1. *Nature* **468**, 696–700.
- Hoeijmakers, J.H. (2009). DNA damage, aging, and cancer. *N. Engl. J. Med.* **361**, 1475–1485.
- Horowitz, M.P., Milanese, C., Di Maio, R., Hu, X., Montero, L.M., Sanders, L.H., Tapias, V., Sepe, S., van Cappellen, W.A., Burton, E.A., Greenamyre, J.T., and Mastroberardino, P.G. (2011). Single-cell redox imaging demonstrates a distinctive response of dopaminergic neurons to oxidative insults. *Antioxid. Redox Signal.* **15**, 855–871.
- Kamel, F., Tanner, C., Umbach, D., Hoppin, J., Alavanja, M., Blair, A., Comyns, K., Goldman, S., Korell, M., Langston, J., et al. (2007). Pesticide exposure and self-reported Parkinson's disease in the agricultural health study. *Am. J. Epidemiol.* **165**, 364–374.
- Lin, E., Cavanaugh, J.E., Leak, R.K., Perez, R.G., and Zigmond, M.J. (2008). Rapid activation of ERK by 6-hydroxydopamine promotes survival of dopaminergic cells. *J. Neurosci. Res.* **86**, 108–117.
- Liu, L., Hsu, S.S., Kalia, S.K., and Lozano, A.M. (2003). Injury and strain-dependent dopaminergic neuronal degeneration in the substantia nigra of mice after axotomy or MPTP. *Brain Res.* **994**, 243–252.
- Mastroberardino, P.G., Orr, A.L., Hu, X., Na, H.M., and Greenamyre, J.T. (2008). A FRET-based method to study protein thiol oxidation in histological preparations. *Free Radic. Biol. Med.* **45**, 971–981.
- Mastroberardino, P.G., Hoffman, E.K., Horowitz, M.P., Betarbet, R., Taylor, G., Cheng, D., Na, H.M., Gutekunst, C.A., Gearing, M., Trojanowski, J.Q., et al. (2009). A novel transferrin/TfR2-mediated mitochondrial iron transport system is disrupted in Parkinson's disease. *Neurobiol. Dis.* **34**, 417–431.
- Mutez, E., Nkiliza, A., Belarbi, K., de Broucker, A., Vanbesien-Mailliot, C., Bleuse, S., Dufloot, A., Comptdaer, T., Semaille, P., Blevaque, R., et al. (2014). Involvement of the immune system, endocytosis and EIF2 signaling in both genetically determined and sporadic forms of Parkinson's disease. *Neurobiol. Dis.* **63**, 165–170.
- Niedernhofer, L.J. (2008). Nucleotide excision repair deficient mouse models and neurological disease. *DNA Repair (Amst.)* **7**, 1180–1189.
- Nouspikel, T. (2008). Nucleotide excision repair and neurological diseases. *DNA Repair (Amst.)* **7**, 1155–1167.
- Pascucci, B., D'Errico, M., Parlanti, E., Giovannini, S., and Dogliotti, E. (2011). Role of nucleotide excision repair proteins in oxidative DNA damage repair: an updating. *Biochemistry (Mosc)* **76**, 4–15.
- Robbins, J.H., Otsuka, F., Tarone, R.E., Polinsky, R.J., Brumback, R.A., and Nee, L.E. (1985). Parkinson's disease and Alzheimer's disease: hypersensitivity to X rays in cultured cell lines. *J. Neurol. Neurosurg. Psychiatry* **48**, 916–923.
- Robinson, M.D., McCarthy, D.J., and Smyth, G.K. (2010). edgeR: a Bioconductor package for differential expression analysis of digital gene expression data. *Bioinformatics* **26**, 139–140.
- Salic, A., and Mitchison, T.J. (2008). A chemical method for fast and sensitive detection of DNA synthesis in vivo. *Proc. Natl. Acad. Sci. USA* **105**, 2415–2420.
- Sanders, L.H., Laganière, J., Cooper, O., Mak, S.K., Vu, B.J., Huang, Y.A., Paschon, D.E., Vangipuram, M., Sundararajan, R., Urnov, F.D., et al. (2014a). LRRK2 mutations cause mitochondrial DNA damage in iPSC-derived neural cells from Parkinson's disease patients: reversal by gene correction. *Neurobiol. Dis.* **62**, 381–386.
- Sanders, L.H., McCoy, J., Hu, X., Mastroberardino, P.G., Dickinson, B.C., Chang, C.J., Chu, C.T., Van Houten, B., and Greenamyre, J.T. (2014b). Mitochondrial DNA damage: molecular marker of vulnerable nigral neurons in Parkinson's disease. *Neurobiol. Dis.* **70**, 214–223.
- Schapira, A.H., Cooper, J.M., Dexter, D., Jenner, P., Clark, J.B., and Marsden, C.D. (1989). Mitochondrial complex I deficiency in Parkinson's disease. *Lancet* **1**, 1269.
- Sepe, S., Payan-Gomez, C., Milanese, C., Hoeijmakers, J.H., and Mastroberardino, P.G. (2013). Nucleotide excision repair in chronic neurodegenerative diseases. *DNA Repair (Amst.)* **12**, 568–577.
- Weeda, G., Donker, I., de Wit, J., Morreau, H., Janssens, R., Vissers, C.J., Nigg, A., van Steeg, H., Bootsma, D., and Hoeijmakers, J.H. (1997). Disruption of mouse ERCC1 results in a novel repair syndrome with growth failure, nuclear abnormalities and senescence. *Curr. Biol.* **7**, 427–439.
- Xu, G., Deng, N., Zhao, Z., Judeh, T., Flemington, E., and Zhu, D. (2011). SAMMate: a GUI tool for processing short read alignments in SAM/BAM format. *Source Code Biol. Med.* **6**, 2.